Set2 methyltransferase facilitates cell cycle progression by maintaining transcriptional fidelity

Raghuvar Dronamraju[1],[†], Deepak Kumar Jha[1],[†], Umut Eser[2], Alexander T. Adams[1], Daniel Dominguez[3], Rajarshi Choudhury[4],[5], Yun-Chen Chiang[5], W. Kimryn Rathmell[5], Michael J. Emanuele[4],[5], L. Stirling Churchman[2] and Brian D. Strahl[1],[5],*

[1]Department of Biochemistry & Biophysics, University of North Carolina School of Medicine, Chapel Hill, NC 27599, USA, [2]Department of Genetics, Harvard Medical School, Harvard University, Boston, MA 02115, USA, [3]Department of Biology, Massachusetts Institute of Technology, Cambridge, MA 02115, USA, [4]Department of Pharmacology, University of North Carolina at Chapel Hill, Chapel Hill, NC 27599, USA and [5]Lineberger Comprehensive Cancer Center, University of North Carolina School of Medicine, Chapel Hill, NC 27599, USA

ABSTRACT

Methylation of histone H3 lysine 36 (H3K36me) by yeast Set2 is critical for the maintenance of chromatin structure and transcriptional fidelity. However, we do not know the full range of Set2/H3K36me functions or the scope of mechanisms that regulate Set2-dependent H3K36 methylation. Here, we show that the APC/C^{CDC20} complex regulates Set2 protein abundance during the cell cycle. Significantly, absence of Set2-mediated H3K36me causes a loss of cell cycle control and pronounced defects in the transcriptional fidelity of cell cycle regulatory genes, a class of genes that are generally long, hence highly dependent on Set2/H3K36me for their transcriptional fidelity. Because APC/C also controls human SETD2, and SETD2 likewise regulates cell cycle progression, our data imply an evolutionarily conserved cell cycle function for Set2/SETD2 that may explain why recurrent mutations of *SETD2* contribute to human disease.

INTRODUCTION

Histone post-translational modifications (PTMs), including acetylation, methylation, phosphorylation, and ubiquitylation, are major contributors to chromatin dynamics and the spatio-temporal regulation of DNA-dependent trans-actions such as transcription, replication and DNA repair (1). These modifications are deposited (written), interpreted (read), and removed (erased) by epigenetic machinery (2–

4), which is often recurrently mutated or overexpressed in human diseases (5). Numerous PTMs occur across the unstructured tail and globular domains of histones (1), yet it is poorly understood how these PTMs (singly or in combination) contribute to chromatin structure and function.

Histone lysine methylation plays a significant role in gene transcription (6). For example, while methylation of histone H3 at lysine 4 (H3K4me) is linked to active transcription and marks active promoters and enhancers, methylation of H3 at lysine 36 (H3K36me) contributes to transcription elongation and marks the transcribed regions of genes (7,8). H3K36 is methylated co-transcriptionally by Set2 and functions, partly, to maintain chromatin structure and prevent inappropriate transcription from cryptic promoters during transcription elongation (9–11). This function of H3K36me is dependent on the recruitment/activation of the Rpd3S histone deacetylase complex (9–11) and inhibition of histone exchange (12,13). Thus, one consequence of disrupting Set2 function is loss of transcriptional fidelity, which leads to reduced life span in *Saccharomyces cerevisiae* and *Caenorhabditis elegans* (14,15). Cryptic transcription can occur in the sense direction, and cryptic transcripts can potentially be translated (16). As well, cryptic transcription can occur in the antisense direction, producing 'Set2-repressed antisense transcripts' (17). Intriguingly, H3K36me also dictates the choice between non-homologous end joining and homologous recombination pathways in DNA double-strand break repair (18–22). Consistent with this function of H3K36me in regulating genome stability, the responsible enzymes that methylate human H3K36 (e.g. NSD2, which mediates H3K36me2, and SETD2, which mediates H3K36me3) are

overexpressed or recurrently mutated in a variety of cancers such as renal, breast, and hematological malignancies (5,15).

Although a requirement for Set2/H3K36me is well established in transcriptional fidelity, and, more recently, in nutrient stress and carbon starvation transcriptional programs (23,24), we sought to determine exactly why such regulation exists and whether Set2/H3K36me might also regulate transcriptional programs that are precisely timed and highly tuned, such as the cell cycle transcriptional program. In this report, we identify a function for Set2-mediated H3K36me in cell cycle control. We show that absence of Set2/H3K36me disrupts cell cycle progression and that the Anaphase Promoting Complex/Cyclosome (APC/C) complex degrades Set2 in a cell cycle-dependent manner. Moreover, deletion of *SET2* causes increased antisense cryptic transcription of cell cycle-regulated genes, and this antisense transcription is correlated with mis-regulated sense transcription. Overall, our results suggest that suppression of cryptic transcription by Set2/H3K36me is a general mechanism to maintain the fidelity of highly tuned and highly regulated transcription programs. Because we found that human SETD2 is similarly cell cycle-regulated in an APC-dependent manner, our results also suggest a conserved and basic function for H3K36me in cell cycle control.

MATERIALS AND METHODS

Strains and plasmids

Unless otherwise indicated, all strains are in BY4741 background. *bub1-kd* (SBY11006) and its corresponding wild-type were a gift from Sue Biggins (Fred Hutchison); the *GAL-CDC20* strain was provided by David Morgan (UCSF). *cdc4-1* and *cdc53-1* were gifts from Jennifer Benanti (UMASSMED, Worcester). An H3–H4 wild-type shuffle strain (FY2162) was a gift from Fred Winston (Harvard University) and H3–H4 (K36A) was a gift from Jerry Workman (Stowers Institute). *SET2* was deleted by gene replacement using the PCR toolkit (*SET2::NAT*). The two D-Boxes in Set2 protein were mutated using site directed mutagenesis using Lightning multisite mutagenesis kit. D-box mutants were integrated at the endogenous *SET2* locus using two-step integration method (25). All yeast strains and their genotypes are listed in Supplementary Table S2.

Immunoblots

Generally, yeast strains were grown to an A_{600} of 0.6–0.8, and whole cell extracts were prepared by the SUMEB protocol (http://research.fhcrc.org/gottschling/en/protocols/yeast-protocols/protein-prep.html). Protein extracts were applied to either 8% (Set2, Clb2) or 15% (H3K36me2/3 and H3) SDS-PAGE gels. Transfers were performed at 45 mA/gel for 1.5 h using a Hoeffer semi-dry apparatus. Immunoblotting was performed at 4°C (overnight) using the following antibody dilutions: H3K36me3, 1:1000 (ab9050); H3K36me2, 1:1000 (Active Motif 39255); H3, 1:5000 (Epicypher 13-0001); Clb2, 1:1000 (Santa Cruz sc-9071); HA, 1:1000 (UNC-Antibody Core HA-C5).

Yeast spotting assays

Indicated strains were grown overnight and 5-fold serial dilutions (starting A_{600} 0.25) of these strains were spotted either on minimal medium lacking uracil or on medium containing benomyl (mitotic inhibitor).

Yeast cell cycle synchronization

Yeast cell cycle synchronization was performed according to Keogh *et al.* (9). Briefly, to arrest cells in G1, α-factor was added to WT and *set2Δ* cells (A_{600} ~0.2–0.3) for 3 h. Microscopy and cell cycle markers such as Clb2 confirmed cell cycle arrest. The cells were washed (twice) and re-suspended in fresh medium, and samples (either for protein or RNA extraction) were taken at indicated time points. For nocodazole arrest, cells were grown to $A_{600} = 0.3$ in medium containing DMSO, and nocodazole was then added to 30 µg/ml for 3 h. Arrest was monitored by the appearance of large budded cells.

Flow Cytometry

Overnight wild-type (BY4741) and *set2Δ* cultures were inoculated at an A_{600} of 0.1 and allowed to grow to no >0.25 absorbance units. α-factor was added to cultures at a concentration of 25 nM, and cells were arrested in G1 for 3 h at 30°C. The cultures were then washed three times in sterile water and released into YPD growth medium. Aliquots of cells were collected and fixed (for at least 24 h at 4°C) in 70% cold ethanol at specified time intervals before proceeding to propidium iodide (PI) staining. Fixed cells were washed (1×) in 50 mM citrate buffer, pH 7.5. After washing, cells were incubated with 250 µg/ml RNAse A at 50°C for 2 h. Proteinase K was then added to 1 mg/ml, and incubation was continued for 2 h at 50°C. Cells were washed once with citrate buffer and resuspended at a density of 2 × 10^6 cells/ml. PI was added to a final concentration of 8 µg/ml, followed by 1–2 h incubation at room temperature, after which 10 000 events were recorded on Accuri C6 flow cytometer.

RNA extraction and RT-PCR

Total RNA was prepared from 10 A_{600} units of mid-log phase cells (WT and set2Δ) using hot acid phenol-chloroform extraction followed by ethanol precipitation. 10 µg of crude RNA was treated with DNAse I (Promega) followed by purification using an RNeasy minikit (Qiagen). 500 ng–1 µg of total RNA was used to synthesize cDNA with the SuperScript II first strand synthesis system (Life Technologies); the cDNA was diluted 1:10–1:50 prior to PCR amplification. For cDNA synthesis, either random hexamer primers or gene-specific forward primers were used to detect the sense and antisense RNA, respectively. Primer sequences are available upon request.

Periodic transcription and gene length analysis

A list of *Saccharomyces cerevisiae* periodic genes was downloaded from Cyclebase (http://www.cyclebase.org/

CyclebaseSearch), and the top 800 periodic genes were selected for subsequent analysis. We defined the periodic and non-periodic genes by selecting the top 800 and the last 1000 genes, respectively. For gene annotations for the NET-seq analysis, we relied on the annotation from Xu *et al.* (2009). The list of genes that give rise to cryptic transcripts in *set2∆* was obtained from Lickwar et al. 2009. Statistical significance for the number of genes between different classes (Figure 1 and Supplementary Figure S1) was calculated by hyper-geometric tests, with 5460 genes serving as the total number of genes expressed in a mitotic cell (26). To identify the functionally enriched classes, the candidate list of genes was subjected to ClueGO analysis in Cytoscape (version 3.4) (27), and functional classes with *P* value less than 0.05 are shown in Figure 1A. For Supplementary Figure S1, DAVID (https://david.ncifcrf.gov) (28) was used to analyze the functional enrichment of either 244 genes (from (14)) or 721 genes (from (29)) that commonly give rise to cryptic transcripts and classes that show a functional enrichment with *P*-value <0.05 (Bonferroni corrected) is shown. Inbuilt R-codes (version 3.3.2) were used to determine the length distribution of periodic genes versus a set of random genes.

Elongating RNAPII occupancy analysis

We obtained NET-seq data for WT and *set2∆* from (30) and converted the data into genome format for efficient retrieval (31). Around each position from –200 bp to +200 bp from TSS and TTS, we used a 50 bp window and recorded the ratio of total sense reads to antisense reads. The average ratio for each position was then calculated by averaging over all periodic and non-periodic genes for WT and *set2∆* datasets. The *P*-values for each position were then calculated by comparing the distributions of sense-antisense ratios using the Kolmogorov–Smirnov test.

Mammalian cell lines and cell cycle analysis

Human renal cell carcinoma 786-O and U2OS cells were acquired from the American Type Culture Collection (Manassas, VA, USA). Cells were cultured in Dulbeccos modified Eagle's medium (DMEM, Gibco/Life Technologies, Carlsbad, CA, USA) supplemented with 10% FBS (Gemini Bio-Products, West Sacramento, CA, USA), non-essential amino acids, L-glutamine, penicillin, and streptomycin. All cultures were maintained at 37°C in 5% CO_2. SETD2-knockout (KO) cells and a genetic complementation with a H3K36me3 active form of SETD2 was previously described (42). For Nocodazole arrest, U2OS cells at 60–70% confluency were synchronized to mitotic phase using addition of 200 ng/ml of nocodazole for 16 h. The mitotic cells were collected by shake off, washed three times with warm media and replated. Cells were trypsinized and collected at each intended time points. Cells were lysed in NETN buffer (150 mM NaCl, 0.5 mM EDTA, 50 mM Tris, pH 7.5, 0.5% NP-40) supplemented with protease and phosphatase inhibitors on ice for 20 min. Immunoblots were performed using the following antibodies at the indicated dilutions: Fzr1 and SETD2 antibodies were purchased form Abcam and used at dilutions of 1:300. CycE (1:5000) and p-Histone H3 (1:1000) antibodies were from Cell Signaling

Technologies. Cyclin A (1:5000), Cyclin B (1:10 000) and Ran (1:8000) antibodies were obtained from Santa Cruz Biotechnology Inc. All antibodies were diluted in 5% milk made in phosphate buffered saline. For Hydroxyurea (HU) synchronization, 786-O and SETD2 knockout and rescue cells were incubated with 1 μM HU for 12 h and released by washing with PBS. The cells were collected at the indicated time, fixed with 70% cold ethanol and stored in –20°C for overnight. Cells were then stained with propidium iodide (PI, 50 μg/ml) for determination of total DNA content and analyzed by flow cytometry. At least 20 000 cells were acquired on Beckman Coulter CyAn ADP (Beckman Coulter, Indianapolis, IN, USA) using 488 nm excitation laser and data were analyzed with FlowJo software (TreeStar, Ashland, OR, USA).

RESULTS

Relationship between gene length, Set2-suppression of cryptic transcription, and cell cycle regulation

During transcription elongation, Set2/H3K36me maintains chromatin structure and prevents cryptic transcription in the wake of RNAPII passage (9–11,13). Prevention of cryptic transcription by Set2 has been linked to lifespan control in multiple organisms and the nutrient stress response in yeast. To determine what other cellular processes might be dependent on Set2 suppression of cryptic transcription, we examined a comprehensive dataset of cryptic transcripts, and their corresponding genes, arising from the absence of Set2 (32). A functional enrichment analysis of this dataset revealed that a significant proportion of the cryptic transcripts in *SET2*-deleted (*set2∆*) cells (429 genes identified with high confidence) was functionally enriched for cell cycle-associated processes, most notably 'cell cycle', 'cell division', 'mitotic cell cycle', and 'cytoskeletal reorganization' (Figure 1A and Supplementary Table S1). Other significantly enriched pathways were 'regulation of cell signaling' and 'response to stress', pathways both consistent with our previous findings (24) and intimately tied to cell cycle progression.

To further understand how these cryptic transcripts are related to the cell cycle, we compared the number of genes that give rise to cryptic transcripts in *set2∆* cells with the number of genes that are transcribed in a highly periodic manner (i.e. the 800 top ranked periodically expressed genes from Cyclebase (http://www.cyclebase.org/CyclebaseSearch) (33). This comparison showed a significant overlap ($P = 0.00548$) between genes that give rise to cryptic transcripts and genes that are periodic (Figure 1B). Recently, Sen *et al.* showed that loss of H3K36me in *S. cerevisiae* and *C. elegans* abrogated transcriptional fidelity and resulted in decreased lifespan. In agreement with our finding that cryptic transcription is over-represented in periodic genes, a functional enrichment analysis of 244 genes identified by Sen *et al.* as giving rise to cryptic transcripts during aging also showed an over-representation of cell cycle-associated genes (Supplementary Figure S1A). In addition, a significant proportion of these 244 genes was also identified as being periodically expressed, as defined by Santos *et al.* (33) (Supplementary Figure S1B). Finally, from a dataset
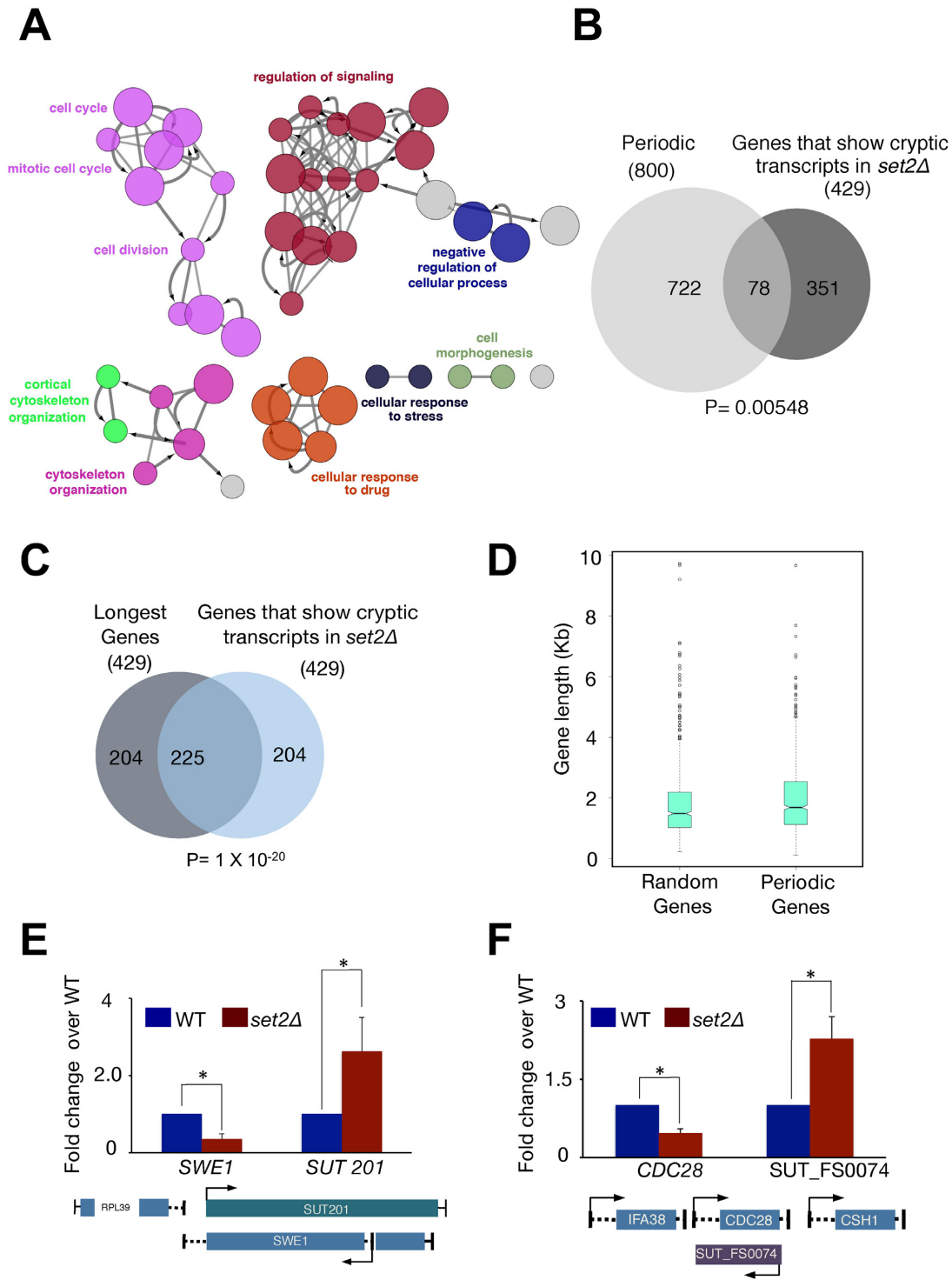
Figure 1. Long genes prone to cryptic transcripts are associated with cell cycle related functions. (**A**) Network analysis, following pathway enrichment analysis, of genes that give rise to cryptic transcript from (32) showing the ontology relationships between the pathways. Genes that give rise to cryptic transcripts (429 genes from Lickwar *et al.* (32)) in *set2*Δ cells reveal an enrichment of these genes with the cell cycle, mitosis, DNA replication and cell polarity. The direction of the arrows shows the ontogeny of related functional categories. (**B**) A Venn diagram comparing genes that are periodic (top 800 from Cyclebase) to those that give rise to cryptic transcripts in *set2*Δ cells reveal a significant overlap (p = 0.00548). (**C**) Venn diagram showing that genes which give rise to cryptic transcription in *set2*Δ cells also tend to be long ($P < 1 \times 10^{-20}$). (**D**) Plot showing the relationship between long genes (800 random genes) and periodic genes (top 800 from Cyclebase) reveal periodic genes tend to be longer than expected by chance ($P < 2.531 \times 10^{-5}$ Kolmogorov–Smirnov test). (**E**) and (**F**) RT-qPCR analysis of sense and antisense transcripts originating from the *SWE1* (*SUT201*) and *CDC28* genes (*SUT_FS0074*), demonstrating the reduced sense transcript levels of *SWE1* and *CDC28* in *set2*Δ cells.

of Pelechano and Steinmetz (29), we again observed a significant over-representation of cell cycle and cell division genes that showed cryptic transcription after loss of *SET2* (Supplementary Figure S1C).

Consistent with a study by the Workman group (34), the analyses above also revealed that genes which give rise to cryptic transcripts are, on average, longer than expected by random chance ($P = 1 \times 10^{-20}$) (Figure 1C). Because a high proportion of genes associated with cryptic transcription is represented by cell cycle-related functions, and these genes also tend to be long, we asked whether periodic genes are themselves longer than expected by chance. Indeed, we found that the top 800 periodic genes are longer than predicted by random chance ($P < 2.531 \times 10^{-5}$) (Figure 1D). Interestingly, mammalian genes involved in the G2-M transition also tend to be longer than expected by chance (35). Collectively, these results indicate that cell cycle-regulated genes tend to be long and, thereby, more dependent than other gene classes on the Set2/Rpd3 pathway to prevent cryptic transcription.

Set2 is required to maintain transcriptional fidelity during cell cycle progression

Because cell cycle genes appear to be highly susceptible to cryptic transcription, we next asked whether Set2/Rpd3S might contribute to regulation of periodic genes by suppressing cryptic antisense transcription. Significantly, several studies have demonstrated the potential of antisense transcripts to directly cause transcriptional interference, especially when an antisense transcript overlaps a sense transcription start site (TSS) (24,36–38). Therefore, we identified key cell cycle-regulated genes that exhibited a stable unannotated transcript (SUT) overlapping the start site of the sense promoter, and this list included key cell cycle regulatory genes such as *FAR1*, *SWE1* and *CDC28*. Notably, an overlapping antisense transcript for *CDC28* is critical in regulating *CDC28* transcription during osmotic stress response (37). We used strand-specific real-time quantitative PCR (RT-qPCR) to measure the sense/antisense transcript abundance of *CDC28* and *SWE1* in asynchronously growing WT and *set2Δ* cells. These measurements revealed that the *CDC28* and *SWE1* sense transcripts were down-regulated in *set2Δ* cells, whereas simultaneously, their corresponding antisense transcripts were upregulated by more than two-fold (Figure 1E and F).

Given the above findings, we next extended our analysis to measure the sense and antisense transcript abundance of periodic genes across the cell cycle in WT and *set2Δ* cells. We selected *FAR1* and *SWE1* for these examinations, as these two genes are dynamically regulated across the cell cycle and possess annotated SUTs that extend to the TSS (Figure 2A and D). In agreement with previous studies, *FAR1* sense transcription was down-regulated upon G1 arrest and release (Figure 2B) (39). In addition, the overlapping *FAR1* SUT (*SUT204*) was cyclically regulated across the cell cycle, with its level being highest when the *FAR1* sense transcript was at its lowest level (Figure 2C). In *set2Δ* cells, however, this pattern was significantly altered with *FAR1* sense and antisense transcript levels being higher

compared with the levels observed in WT cells (Figure 2B and C).

We next examined the cell cycle transcript profile of *SWE1* and its antisense transcript *SUT201* (Figure 2D)*. As expected, the *SWE1* transcript level was up-regulated upon entry into S-phase (30 min), after which it returned to baseline level (Figure 2E) (40). Similar to *FAR1*, we found that the antisense *SUT201* transcript abundance was also periodically expressed and anti-correlated with the *SWE1* levels across the cell cycle (Figure 2F). In contrast, *SWE1* levels were significantly reduced during S-phase in *set2Δ* cells, and this reduced level persisted after cells exited S-phase, compared with WT cells in which the *SWE1* transcript was down-regulation post S-phase. However, and somewhat similar to *SUT204*, the levels of *SUT201* showed aberrant regulation across the cell cycle in *set2Δ* cells (Figure 2F). Interestingly, the anti-correlation found with these sense and antisense transcripts were largely restricted to the times of peak expression of these genes. Together, these results document a sense/antisense anti-correlation of periodically expressed genes in WT cells, a finding that agrees with others (41). They also suggest that Set2-dependent suppression of antisense transcripts has an important function in fine-tuning the levels of sense transcripts across different phases of cell cycle.

We next sought determine the effect of uncoupling antisense transcription from sense transcription across the cell cycle for one of the aforementioned genes. To achieve uncoupling, we inserted a ∼2 kb *KANMX* cassette into the 3′-end of the *FAR1* gene, thereby physically displacing *SUT204* away from the *FAR1* TSS (Figure 2G). Without the cassette insertion, and as observed in Figure 2B, *FAR1* sense transcript level decreased upon entry into the S-phase, then became lower in the S- and G2-phase, and began peaking in the M-phase (Figure 2H). Significantly, insertion of the *KANMX* cassette caused a drastic increase in the expression level of the *FAR1* sense transcript at the 60 min time interval; this increase was subsequently down-regulated to WT levels by 90 min. Across the cell cycle, the displaced *FAR1* antisense transcript, *SUT204*, was significantly decreased compared with the WT control transcript, suggesting that this antisense transcript is key to regulation of the *FAR1* sense transcript (Figure 2I).

Because antisense SUTs can potentially affect sense transcription of periodically expressed genes, we asked whether antisense cryptic unstable transcripts (CUTs), that are also regulated by the Set2/Rpd3 pathway (30), might also confer a similar fate upon cell cycle-regulated gene sense transcription. Significantly, Castelnuovo *et al*. reported that specific CUTs, when not terminated properly by Nrd1/Nab3/Sen1-dependent termination pathway, harbor a similar capability to suppress sense transcription (42). To explore if antisense transcripts are altering sense transcription, we analyzed NET-seq data generated from WT, *set2Δ*, and *rco1Δ* cells (30) and determined the occurrence and effect of antisense CUTs on transcription of periodic and non-periodic genes. Consistent with expectations, the absence of Set2 or Rco1 led to genome-wide increases in CUT formation at the 5′- and 3′-ends of genes (Supplementary Figure S2 and data not shown). However, the increases in CUT formation occurred irrespective of whether or not the genes were ex-
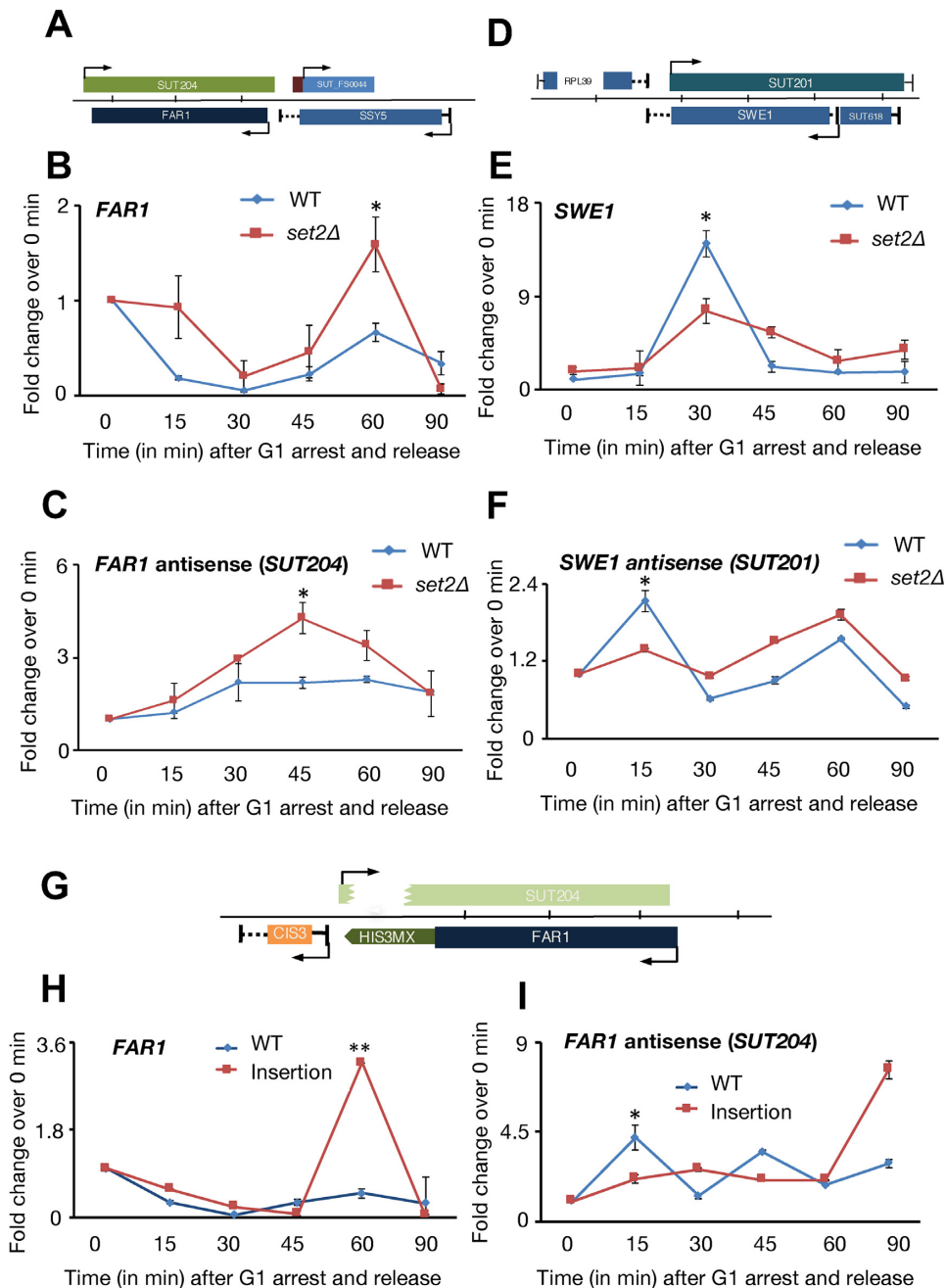
Figure 2. The transcriptional fidelity of cell cycle-regulated genes is maintained by Set2. (**A**) Diagrammatic representation of the *FAR1* locus and its corresponding antisense stable un-annotated transcript (*SUT204*). (**B**) qRT-PCR showing the absence of *SET2* results in mis-regulation of the levels of both sense and antisense *FAR1* transcripts. (**C**) *FAR1* antisense transcript, *SUT204*, is increased in *set2Δ* cells at all points across the cell cycle, as assessed by qRT-PCR. (**D**) Schematic representation of the genomic locus of *SWE1* and its corresponding antisense transcript, *SUT201*. (**E**) Loss of *SET2* results in the mis-regulation in the levels of *SWE1* sense transcript (compare the levels of *SWE1* transcript at 30 and 45 min between WT and *set2Δ*). (**F**) qRT-PCR of *SWE1* antisense transcript *SUT201*, shows altered expression kinetics in *set2Δ* cells. (**G**) Schematic representation of the *FAR1* locus with an insertion of a 2 kb *KANMX* cassette to displace the *SUT204* from the *FAR1* 3′ end (**H**) qRT-PCR to detect the levels of *FAR1* transcript in a strain that lacks the 2 kb *KANMX* cassette and showing a similar down-regulation of *FAR1* as in Figure 2B. (**I**) levels of *SUT204* in a strain containing the 2 kb *KANMX* cassette showing partial abrogation of the transcript. The data in all the above experiments are represented as the standard deviations of three biological replicates with three technical replicates in individual experiments. The statistical significance was calculated using paired t test (* represents *P* value <0.01).

pressed periodically, revealing a broad role for Set2 in suppressing CUT formation.

We further examined the NET-seq data to assess how the absence of Set2 specifically affects CUT formation from periodically expressed genes, and whether changes in CUT formation are associated with decreased sense transcription. The NET-seq data revealed that transcription of many important cell cycle genes, including *CDC5*, *CDC20* and *CLB2*, was significantly down-regulated in a *set2Δ* strain compared with the WT; however, these decreases did not correlate with increases in CUT formation (Supplementary Figure S3). Conversely, *DBF2*, a key periodically regulated gene required for mitotic exit, showed a striking increase in its 3′ antisense transcript (*CUT613*) that correlated with a decrease in sense transcription of *DBF2*, suggesting that this antisense transcript might be involved in regulating sense transcription (Figure 3A and B). To investigate the possibility of antisense-mediated regulation of *DBF2*, we measured its sense transcript and CUT across the cell cycle (Figure 3C and D). Remarkably, *CUT613* was up-regulated in *set2Δ* cells as reported (30), and its up-regulation occurred in G2/M, which is when *DBF2* is normally expressed. Significantly, increased CUT formation in *set2Δ* cells was associated with decreased sense production at all time points, as assessed by strand-specific qRT-PCR (Figure 3C and D). While these results suggest that the decrease in *DBF2* might be mediated through transcriptional interference of increased C*UT613* expression, we cannot rule out the possibility that *DBF2* expression functions to suppress *CUT613* expression. Nonetheless, these findings further support a function for Set2 in reinforcing the transcriptional fidelity of genes that are key to cell cycle regulation.

Set2 and H3K36 methylation are required for timely progression through the cell cycle

Having established that Set2 is required for proper expression of cell cycle-regulated genes, we next asked whether deletion of *SET2* would lead to cell cycle progression defects. To address this question, we arrested WT and *set2Δ* cells with α-factor, released them into fresh medium, and collected cells at the indicated time points for flow cytometry (Figure 4A). Consistent with our results showing disruption of cell cycle regulated gene transcription upon *SET2* loss, *set2Δ* cells displayed a substantial delay (∼15 min) in the release from G1 into S-phase (Figure 4B). In addition to this delayed entry into S-phase, our flow cytometry studies revealed that the number of cells in the S-phase was lower in *set2Δ* cells compared with WT, suggestive of a faster progression through S phase (Figure 4C). To confirm that absence of Set2 leads to faster S-phase progression, we arrested WT and *set2Δ* cells for 2 h with 200 mM hydroxyurea (HU), washed the cells and released them into fresh medium, and collected time points. In this experiment, *set2Δ* cells exited S-phase 15 min faster than the WT cells (Supplementary Figure S5), further confirming a function for Set2 in different phases of the cell cycle. In agreement with these findings, results from Biswas *et al.* also showed that Set2 inhibits DNA replication (43). Further support for this was also recently provided by Pai *et al.*, who showed that Set2 in *S. pombe* is required for efficient DNA
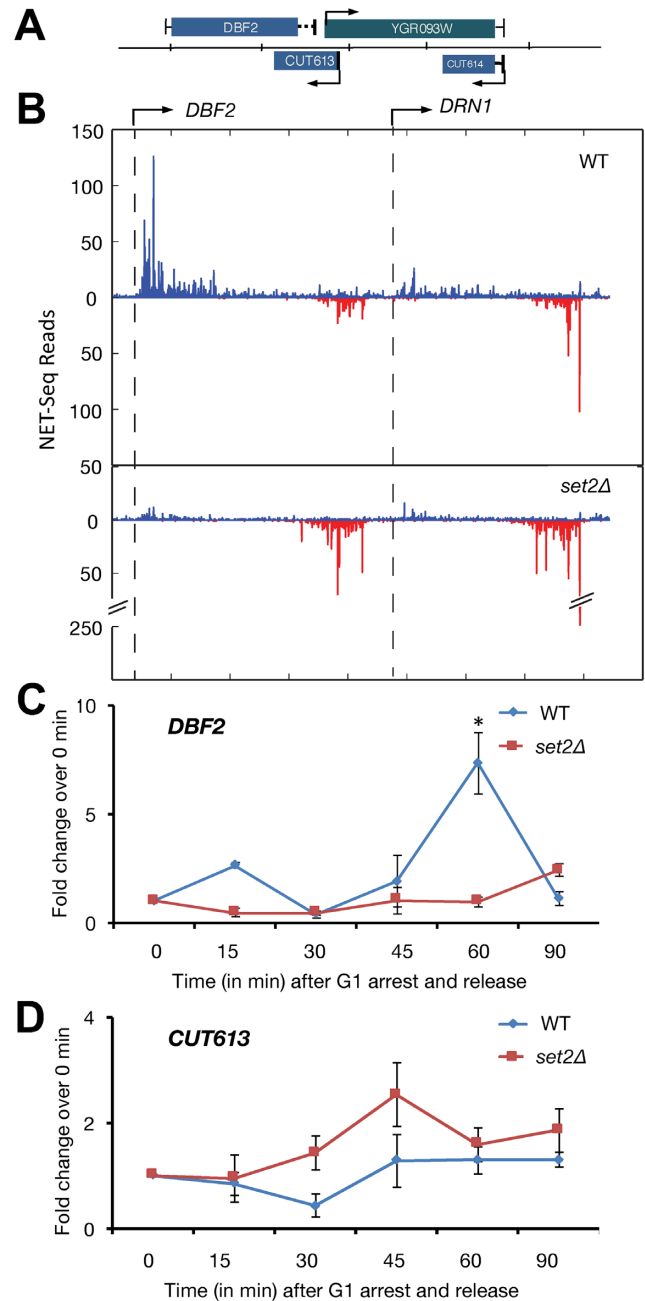

Figure 3. Set2 is required to repress cryptic unstable transcripts at the cell cycle-regulated *DBF2* locus. (**A**) Schematics of *DBF2* gene organization alongside its neighboring gene (*DRN1*) and the cognate antisense transcripts *CUT613* and *CUT614*, respectively. (**B**) Genome browser shot of the sense and antisense transcripts originating from the WT and *set2Δ* cells. (**C**) and (**D**) WT or *set2Δ* cells were arrested with α-factor, then released into fresh medium, after which samples were collected at indicated time points for strand-specific qRT-PCR. Results show that as *DBF2* levels increase in G2/M, its corresponding antisense *CUT613* is also detectable. Absence of Set2 results in significant increase in *CUT613* production that correlates with sense decrease, suggesting that *CUT613* antisense transcripts can interfere with sense transcription. The data in are represented as the standard deviations of three biological replicates with three technical replicates in individual experiments. Statistical significance was calculated using paired t test (* represents *P* value <0.01).
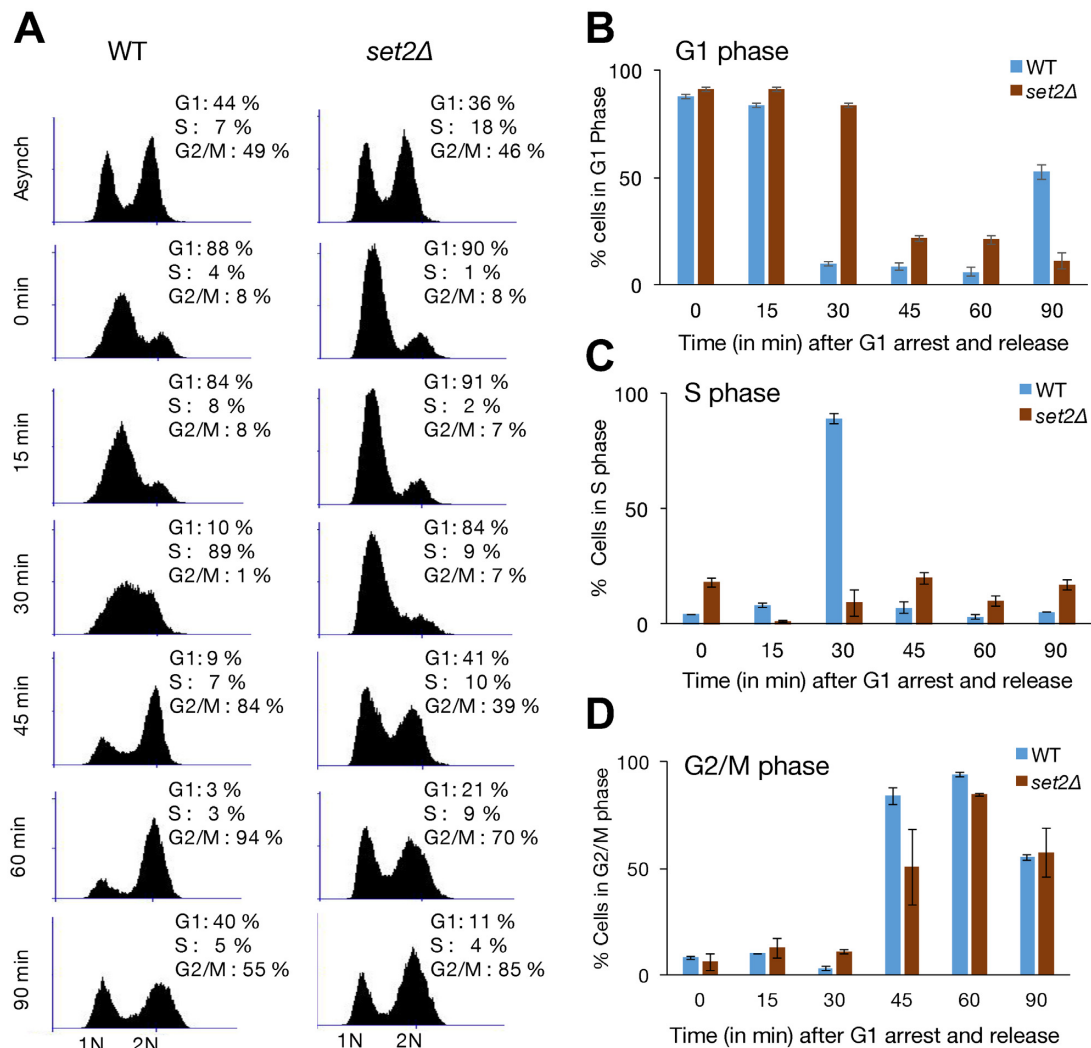
Figure 4. Loss of Set2 and H3K36 methylation abrogates yeast cell cycle progression. (**A**) Representative flow cytometry profiles of WT and *set2*Δ cells after α-factor arrest and release, which reveal defects in the ability of *set2*Δ cells to properly progress through the cell cycle. Comparison of the profiles at 30, 45 and 60 min after release in G1 show *set2*Δ cells have a delayed entry into S-phase, which then progresses faster than that observed for WT cells. (**B–D**) Quantification of multiple flow cytometry profiles of WT and *set2*Δ cells (*n* > 3) in which G1, S and G2/M cells from WT and *set2*Δ cells are counted.

replication by regulating the MBF transcriptional program ([44](#)). However, the mechanistic basis by which Set2 controls S-phase progression and proper checkpoint activation remains unknown. Finally, although G1- and S-phase progression were perturbed, we did not observe any significant changes in the fraction of cells in the G2/M-phase of cell cycle (Figure [4](#)D). To determine whether the *set2*Δ cell cycle delay was a catalysis-dependent function directed toward the H3K36 residue, we examined a strain in which H3K36 was mutated to alanine (H3K36A), hence, K36 could not be methylated. Like the absence of Set2, loss of H3K36 methylation in the H3K36A strain caused a similar delay in release from G1 (Supplementary Figure S4).

Set2/SETD2 are regulated in temporal manner during cell cycle progression

Because of the unexpected connection between Set2 and the cell cycle, we asked whether Set2 itself might be subject to cell cycle regulation. Surprisingly, as assayed by immunoblot analysis after α-factor arrest and release, we found that Set2 levels were lower in the G1- and S-phases compared with G2/M, suggesting that Set2 is specifically targeted for destruction after M-phase (Figure [5](#)A). To test this possibility in an independent way, we performed a nocodazole arrest-release experiment and examined Set2 levels after release from metaphase arrest. Strikingly, and consistent with our α-factor arrest-release results, Set2 accumulated after nocodazole treatment, but its levels decreased upon release from nocodazole (G2/M) arrest (Figure [5](#)B). Furthermore, Set2 levels remained low across the G1- and S-phases, as assessed by immunoblot analysis for
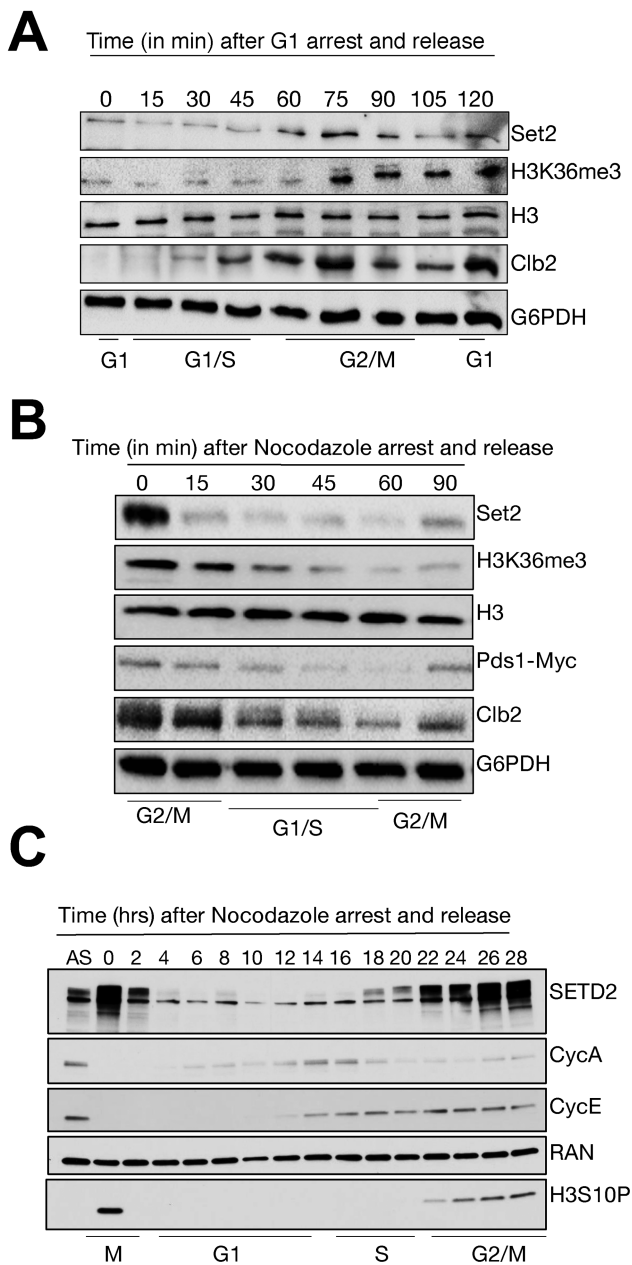
Figure 5. Yeast and human Set2 are cell cycle regulated proteins. (**A**) Set2 protein is cell cycle regulated. WT and *set2Δ* cells were arrested in the G1 phase using α-factor and released into fresh medium. Whole cell extracts were prepared at indicated time points and probed for Set2, H3, H3K36me3, Clb2 (marker for cell cycle progression) and G6PDH (total protein loading). (**B**) Set2 protein levels are down-regulated during progression through mitosis and mitotic exit. Whole cell extracts were prepared at designated time points after release from nocodazole. WT cells were released into fresh medium and immunoblotted for Set2, Clb2 (a marker for cell cycle progression), Pds1 (a marker for metaphase to anaphase transition) and G6PDH (total protein loading control). Analogous to Set2, H3K36me3 levels similarly change across the cell cycle, as analyzed by immunoblotting for H3K36me2/me3, and anti-H3 (loading control). (**C**) Human SETD2 is a cell cycle regulated protein. U2OS cells were synchronized using nocodazole, collected at indicated time points, and immunoblotted for SETD2. CycA, CycE and H3S10P serve as markers for different cell cycle stages, whereas RAN was used as a loading control.

Set2 and the control G2/M markers Clb2 and Pds1 (Figure 5B). We also observed that the level of Set2 began to increase at 90 min after release from nocodazole (Figure 5B, last lane). These data strongly suggest that Set2 turnover occurs in a cell cycle-dependent manner. Importantly, the regulation of Set2 was not due to a defect in *SET2* transcription because *SET2* transcript levels were not cell cycle-regulated (Supplementary Figure S6). A further analysis of H3K36me3 levels across the cell cycle agreed with our findings for Set2, with the highest methylation levels occurring in G2/M and the lowest levels in G1 and S-phase (Figure 5A). Intriguingly, loss of H3K36me3 after nocodazole release was delayed relative to the rapid loss of Set2, consistent with H3K36me being removed secondarily by H3K36 demethylases (45).

To ascertain whether Set2 regulation across the cell cycle is evolutionarily conserved, we performed a nocodazole arrest-release experiment with U2OS cells and immunoblotted for human SETD2 plus H3S10p, CycA and CycE (S-phase markers of cell cycle progression); RAN served as a loading control. Similar to yeast Set2, we found that human SETD2 was cell cycle-regulated, with increased accumulation during mitosis (Figure 5C).

Set2/SETD2 are targeted for destruction by the APC/C complex

To identify the cell cycle-associated degradation machinery that targets Set2, we screened temperature-sensitive alleles of members of the Skp-Cullin-F-box (SCF) containing complex and the anaphase-promoting complex/cyclosome (APC/C) to determine which, if any, is involved in Set2 degradation. Thermal inactivation of temperature sensitive SCF members (*CDC4* and *CDC53*) in asynchronously growing strains did not alter Set2 protein abundance (Supplementary Figure S7A). In contrast, inactivation of APC/C complex members did affect Set2 abundance. Specifically, thermal inactivation of Cdc23 of the APC/C complex, followed by a cycloheximide chase, prevented the rapid turnover of Set2 observed in WT cells (Figure 6A).

APC/C interacts with either Cdc20 or Cdh1 to form two distinct complexes (APC/C^{Cdc20} and APC/C^{Cdh1}) that function during G2/M- and G1-phases of the cell cycle respectively (46). Thus, we next asked whether one or both complexes might target Set2 for degradation. Kinetics of Set2 degradation (using cycloheximide chase) were not altered upon deletion of *CDH1*, thus ruling out its involvement (Figure 6B). Because a *CDC20* deletion is not viable, we used a *GAL*-inducible form of *CDC20*, whose expression could be turned on and off by the addition of galactose or dextrose, respectively. When *CDC20* expression was off (*i.e.* by dextrose), we observed a significant increase in the protein levels of Set2 and Clb2, a known substrate of APC/C^{Cdc20} (Figure 6C). In addition, APC/C^{Cdc20} is negatively regulated by Bub1-dependent phosphorylation (47). Thus, we used a *bub1Δ* and a Bub1 kinase-dead mutant to increase APC/C^{Cdc20} activity. In both strains, we found that Set2 and H3K36me3 were significantly reduced, supporting the conclusion that Set2 is targeted for degradation by the APC/C^{Cdc20} complex (Figure 6D and Supplementary
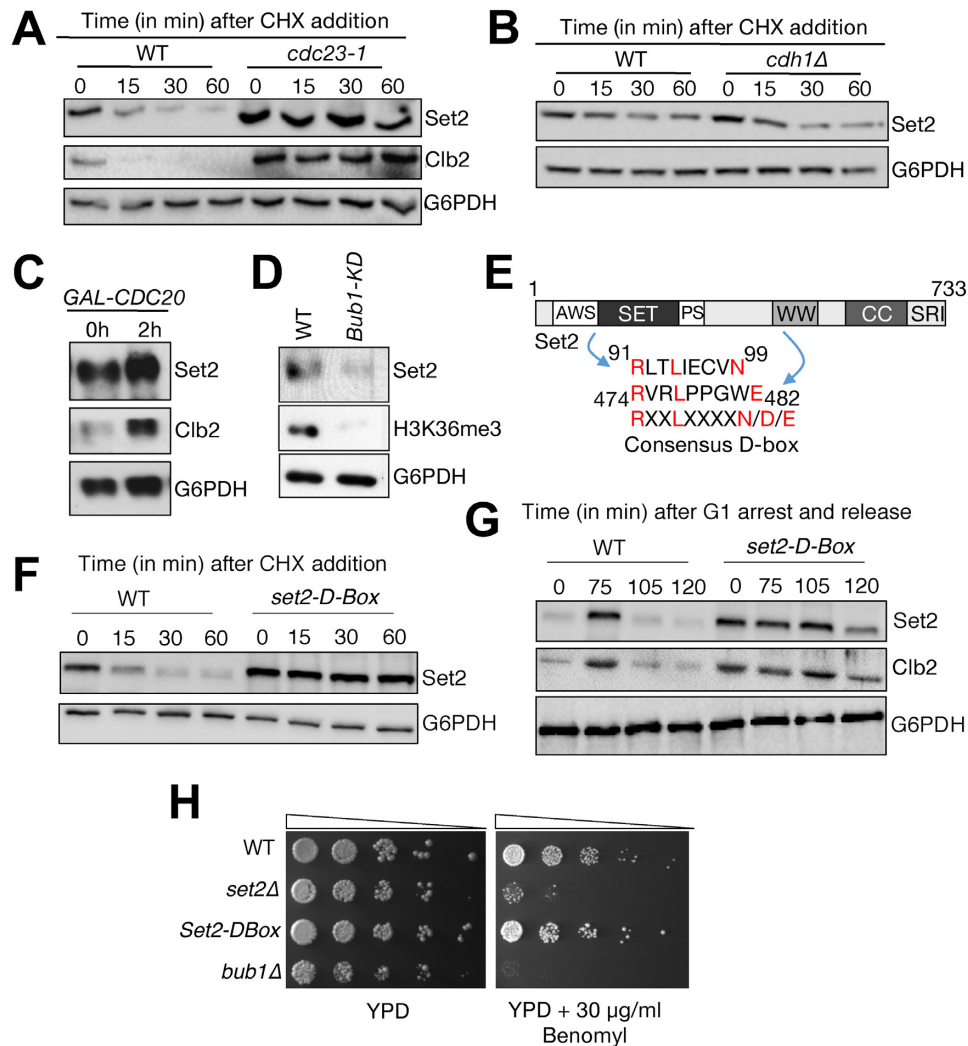
Figure 6. The Anaphase Promoting Complex (APC) promotes Set2 protein turnover across the cell cycle. (**A**) Compromised APC/C function stabilizes Set2 protein levels. Cycloheximide chase experiments were performed using a WT or APC mutant allele (*cdc23–1*) after shift to restrictive temperature (37°C), and cell extracts were immunoblotted for Set2. G6PDH was used as a loading control. (**B**) Set2 is not regulated by APC/C^{Cdh1}. Cycloheximide chase experiments were performed as described in panel (A) in WT and *CHD1* deleted cells (*cdh1△*) to detect the rate of Set2 loss. (**C**) Set2 is regulated by the APC/C^{Cdc20}. A *GAL-CDC20* strain was grown in dextrose for 2 h to shut off expression of *CDC20*, and protein extracts were immunoblotted to probe for Set2, Clb2 and G6PDH. (**D**) An immunoblot showing the decrease in the levels of Set2 and H3K36me3 in a strain that contains a kinase-dead allele of *BUB1*, a checkpoint kinase that negatively regulates *CDC20*. (**E**) Representation of Set2 protein showing the domains and two putative D-boxes in the protein sequence. For comparison, a canonical D-box sequence is shown. (**F**) Mutation of the conserved D-box residues in Set2 (RXXL → AXXA) enhances Set2 stability. Cycloheximide chase experiments were performed at the indicated time points on WT and the D-box mutant strains and probed for Set2 and G6PDH. (**G**) Set2 protein levels become uncoupled from cell cycle regulation upon D-box mutation. Lysates were prepared from WT and D-Box mutants of Set2 post G1 arrest and released at indicated time points. Lysates were probed for Set2, Clb2 and G6PDH. (**H**) Appropriate turnover of Set2 protein is required for proper response to mitotic poison, benomyl. Five-fold serial dilutions of indicated strains were spotted on either SC-Ura or SC-Ura with benomyl (30 μg/mL).

Figure S7B). Consistent with this finding, the levels of Set2 and the metaphase-to-anaphase transition marker Pds1 decreased within the first 15 min after release from nocodazole arrest (Figure 5A).

To pinpoint more precisely how Set2 is targeted for destruction, we analyzed the Set2 protein sequence and found two canonical D-box consensus motifs (RxxLxxxxN/D/E) that are associated with APC/C^{Cdc20} targets (47) (Figure 6E). To determine whether these putative D-boxes control the stability of Set2, we mutated both D-boxes (changing RxxL to AxxA in each putative consensus sequence site)

and replaced endogenous WT with mutant *SET2* at its locus. We assessed the stability of WT and D-box mutant form of Set2 (*set2D-Box*) using cycloheximide chase assays as described above. Mutation of the Set2 D-boxes led to stabilization of Set2 protein (Figure 6F), confirming that the D-boxes are targets of APC/C^{Cdc20}. To determine whether the D-Box mutants of Set2 were defective in the cell cycle pattern of protein degradation like that depicted in Figure 5A, we arrested the WT and *set2D-Box* mutant strains with α-factor and assessed the dynamics of Set2 abundance at different points. We used 0, 75, 105 and 120 min time intervals

because they allowed us to directly visualize the WT and D-box mutant proteins on the same immunoblot, without having to compare Set2 among different gels. After G1 arrest and release, the level of Set2 was highest at the 75 min (G2/M) interval (Figure 6G), consistent with Figure 5A. As expected, the D-box mutants showed an increase in overall Set2 protein level and Set2 was not degraded in a manner similar to WT. These observations strongly suggest that degradation of Set2 is coupled with cell cycle progression. Finally, and consistent with a function for Set2 in mitosis, we observed that deletion of *SET2* rendered cells sensitive to benomyl, a microtubule poison that arrests cells in G2/M (Figure 6H). Interestingly, compared with WT cultures, under normal conditions, stabilization of Set2 (by mutating the D-boxes) conferred a slight growth advantage and an increased resistance to benomyl (Figure 6H).

To determine whether human SETD2 is also regulated by APC/C, we over-expressed the human APC/C-Cdh1 homolog (*FZR1*) because SETD2 did not appear to possess a putative D-box, but it did exhibit a putative KEN-box at residues 2033–2035 (47). This experiment showed that SETD2 levels were reduced after *FZR1* over-expression, and SETD2 levels were restored by the proteasome inhibitor MG132 (Supplementary Figure S8A). Furthermore, down-regulation of *FZR1* increased SETD2 levels (Supplementary Figure S7A). Finally, and consistent with what we observed in strains lacking Set2, SETD2 knock-out from 786-O cell lines caused a faster progression through S-phase, which was rescued by over-expression of an N-terminal truncated form of SETD2 (tSETD2) that functionally complements a SETD2 deletion (Supplementary Figure S8B) (48). These data revealed a remarkable conservation in APC/C targeting of Set2 and SETD2 for destruction, and the results imply an important and conserved function for H3K36me in cell cycle regulation.

A non-degradable form of Set2 causes transcriptional defects in cell cycle regulated genes

Because mutation of the two D-boxes in Set2 conferred stability and uncoupled the protein from cell cycle regulation, we took advantage of the D-box mutant alleles to assess the consequence of a stabilized Set2 for sense and antisense transcription of cell cycle regulator genes. Similar to our approach in Figure 2, we performed stranded qRT-PCR to measure the sense and antisense transcript levels of *FAR1* and *SWE1* (Supplementary Figure S9A and S9D). In agreement with Figure 2, *set2Δ* cells showed defects in the regulation of the *FAR1* and *SWE1* sense transcripts compared with their WT expression patterns (Supplementary Figure S9B and S9C). In contrast, however, the sense transcription levels of *FAR1* and *SWE1* were improperly regulated across the cell cycle in the *set2D-Box* mutant, as compared with that observed in both WT and *set2Δ* cells (Supplementary Figure S9B and S9C). Along with the defects observed in sense transcription, the antisense transcripts *SUT204* and *SUT201* were also mis-regulated in the *Set2* D-Box mutant strain, as compared with their transcription in WT and *set2Δ* cells (Supplementary Figure S9E and S9F). These results showed that cell cycle regulation of Set2 is essential to maintain chromatin integrity and optimal sense/antisense transcript levels.

DISCUSSION

Our findings reveal a new link between Set2/SETD2 and the cell cycle. We showed that the function of Set2 in the cell cycle is catalysis-dependent, and Set2 functions, at least partly, by preventing aberrant antisense transcription that likely causes transcriptional interference within cell cycle regulator genes (see model in Figure 7). Intriguingly, cell cycle genes tend to be long, which may explain why they are more dependent for their regulation on the Set2/H3K36me pathway. Our findings suggest a model wherein Set2 methylation suppresses the generation of cryptic transcripts (i.e. CUTs and SUTs) that would otherwise interfere with the normal periodic regulation of cell cycle regulator genes. This model of transcriptional interference agrees with several recent studies showing the interference potential of neighboring antisense transcripts (24,36–38,49). Furthermore, our model also posits that other chromatin regulators that suppress antisense or cryptic transcription may be crucial regulators of the cell cycle. Consistent with this idea, a functional classification (DAVID) analysis of genes that give rise to cryptic transcripts in *SPT6* and FACT mutants (*spt6-1004* and *spt16-197*) (16) showed that the most highly represented functional categories were related to 'cell cycle', 'DNA replication', and 'mitosis' (data not shown). We further speculate that such regulation of (sense) mRNAs by associated (antisense) ncRNAs is a general feature of coordinated gene expression programs in other aspects of cellular biology, for example, during metabolic flux. This idea agrees with a recent report that antisense long ncRNAs regulate the induction kinetics of genes that regulate glucose to galactose switching—a switch that involves lncRNA mediated deposition of H3K36 methylation (50).

Grosso *et al.* reported that, in SETD2 mutant tumors, there was widespread transcriptional read-through (51), a manifestation of disrupted transcriptional fidelity that impacted neighboring gene expression in clear cell renal carcinoma (ccRCC). In addition, Park *et al*. reported another direct connection between SETD2 and mitosis, wherein cytoplasmic methylation of tubulin by SETD2 maintained genome stability by promoting proper chromosome segregation (52). Consistent with this observation, our results show that SETD2 levels are highest during mitosis and are down-regulated upon entry into G1, an observation that mirrors budding yeast (Figure 5). Our results also show that *set2Δ* cells are sensitive to the mitotic poison benomyl (Figure 6); likewise, *Schizosaccharomyces pombe set2Δ* cells are sensitive to the mitotic poison thiabendazole (53), suggesting that the function of Set2 in mitosis is conserved. Although it is not known whether Set2 catalyzes methylation of a non-histone substrate in budding yeast, our results using a non-methylatable form of H3K36 strongly suggest that the function of Set2 in cell cycle control is mediated (principally) by histone methylation.

Our discovery that yeast and human Set2 are targeted for destruction by the APC/C complex also implies that Set2 and H3K36me regulate the reinforcement of transcriptional fidelity differently across different phases of the cell cycle.
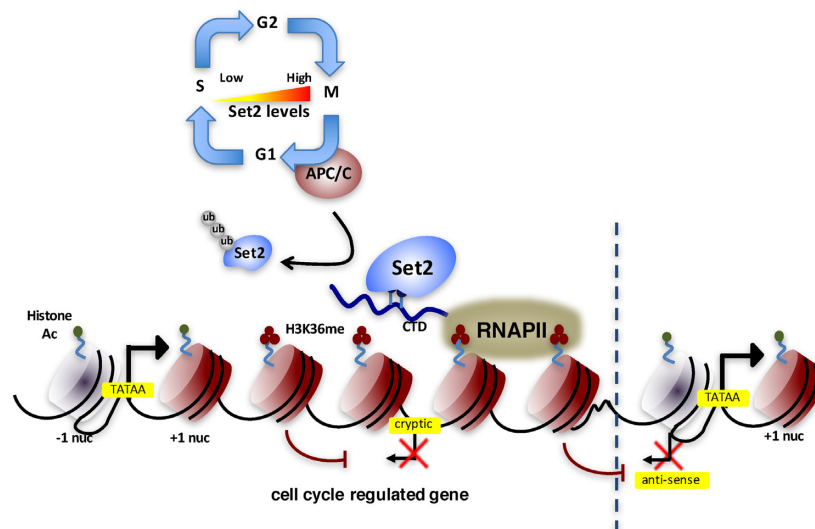
Figure 7. Model for the function of Set2 in regulating the cell cycle by maintaining transcriptional fidelity. In WT cells, Set2-dependent H3K36 methylation is required for the recruitment/activation of the Rpd3S histone deacetylase complex, which maintains a repressed chromatin state that is refractory to pervasive cryptic transcription. Our results show that Set2 protein and H3K36me levels are cell cycle regulated, with lowest levels in the G1- and S-phases and highest in the G2/M-phase. In addition, we found that Set2 and H3K36 methylation is required for the proper expression of cell cycle regulated genes that tend to be long and highly dependent on Set2. Because Set2/H3K36me levels fluctuate across the cell cycle, we speculate that these changing levels fine-tune the levels of cryptic transcription across the cell cycle to allow for optimal expression of genes required for transition through the different cell cycle phases.

This reinforcement of transcriptional fidelity is disrupted when Set2 protein is stabilized by mutating its D-boxes. Interestingly, mutations in the Set2 D-boxes also altered, albeit slightly, the benomyl sensitivity of cells (Figure 6G), suggesting a function of Set2 turnover in regulation of the cell cycle. Although not directly tested here, it is nonetheless important to determine why Set2 and SETD2 are targeted by the APC/C complex. We envision that some of the tumor-promoting functions of mutant SETD2 in ccRCC and other relevant tumors may be a combination of loss of transcriptional fidelity of cell cycle regulators plus misregulation of non-histone targets of SETD2 such as tubulin.

SUPPLEMENTARY DATA

Supplementary Data are available at NAR Online.

ACKNOWLEDGEMENTS

FUNDING

REFERENCES

1. Pirrotta,V. (2016) The necessity of chromatin: a view in perspective. *Cold Spring Harbor Perspect. Biol.*, **8**, a019547.
2. Gardner,K.E., Allis,C.D. and Strahl,B.D. (2011) Operating on chromatin, a colorful language where context matters. *J. Mol. Biol.*, **409**, 36–46.
3. Rothbart,S.B. and Strahl,B.D. (2014) Interpreting the language of histone and DNA modifications. *Biochim. Biophys. Acta*, **1839**, 627–643.
4. Bannister,A.J. and Kouzarides,T. (2011) Regulation of chromatin by histone modifications. *Cell Res.*, **21**, 381–395.
5. Lawrence,M.S., Stojanov,P., Mermel,C.H., Robinson,J.T., Garraway,L.A., Golub,T.R., Meyerson,M., Gabriel,S.B., Lander,E.S. and Getz,G. (2014) Discovery and saturation analysis of cancer genes across 21 tumour types. *Nature*, **505**, 495–501.
6. Patel,D.J. (2016) A structural perspective on readout of epigenetic histone and DNA methylation marks. *Cold Spring Harbor Perspect. Biol.*, **8**, a018754.
7. Strahl,B.D., Grant,P.A., Briggs,S.D., Sun,Z.W., Bone,J.R., Caldwell,J.A., Mollah,S., Cook,R.G., Shabanowitz,J., Hunt,D.F. *et al.* (2002) Set2 is a nucleosomal histone H3-selective methyltransferase that mediates transcriptional repression. *Mol. Cell. Biol.*, **22**, 1298–1306.
8. Wozniak,G.G. and Strahl,B.D. (2014) Hitting the 'mark': interpreting lysine methylation in the context of active transcription. *Biochim. Biophys. Acta*, **1839**, 1353–1361.
9. Keogh,M.C., Kurdistani,S.K., Morris,S.A., Ahn,S.H., Podolny,V., Collins,S.R., Schuldiner,M., Chin,K., Punna,T., Thompson,N.J. *et al.* (2005) Cotranscriptional set2 methylation of histone H3 lysine 36 recruits a repressive Rpd3 complex. *Cell*, **123**, 593–605.

10. Carrozza,M.J., Li,B., Florens,L., Suganuma,T., Swanson,S.K., Lee,K.K., Shia,W.J., Anderson,S., Yates,J., Washburn,M.P. *et al.* (2005) Histone H3 methylation by Set2 directs deacetylation of coding regions by Rpd3S to suppress spurious intragenic transcription. *Cell*, **123**, 581–592.

11. Joshi,A.A. and Struhl,K. (2005) Eaf3 chromodomain interaction with methylated H3-K36 links histone deacetylation to Pol II elongation. *Mol. Cell*, **20**, 971–978.

12. Smolle,M., Venkatesh,S., Gogol,M.M., Li,H., Zhang,Y., Florens,L., Washburn,M.P. and Workman,J.L. (2012) Chromatin remodelers Isw1 and Chd1 maintain chromatin structure during transcription by preventing histone exchange. *Nat. Struct. Mol. Biol.*, **19**, 884–892.

13. Venkatesh,S., Smolle,M., Li,H., Gogol,M.M., Saint,M., Kumar,S., Natarajan,K. and Workman,J.L. (2012) Set2 methylation of histone H3 lysine 36 suppresses histone exchange on transcribed genes. *Nature*, **489**, 452–455.

14. Sen,P., Dang,W., Donahue,G., Dai,J., Dorsey,J., Cao,X., Liu,W., Cao,K., Perry,R., Lee,J.Y. *et al.* (2015) H3K36 methylation promotes longevity by enhancing transcriptional fidelity. *Genes Dev.*, **29**, 1362–1376.

15. McDaniel,S.L. and Strahl,B.D. (2017) Shaping the cellular landscape with Set2/SETD2 methylation. *Cell. Mol. Life Sci.: CMLS*, **74**, 3317–3334.

16. Cheung,V., Chua,G., Batada,N.N., Landry,C.R., Michnick,S.W., Hughes,T.R. and Winston,F. (2008) Chromatin- and transcription-related factors repress transcription from within coding regions throughout the Saccharomyces cerevisiae genome. *PLoS Biol.*, **6**, e277.

17. Venkatesh,S., Li,H., Gogol,M.M. and Workman,J.L. (2016) Selective suppression of antisense transcription by Set2-mediated H3K36 methylation. *Nat. Commun.*, **7**, 13610.

18. Pfister,S.X., Ahrabi,S., Zalmas,L.P., Sarkar,S., Aymard,F., Bachrati,C.Z., Helleday,T., Legube,G., La Thangue,N.B., Porter,A.C. *et al.* (2014) SETD2-dependent histone H3K36 trimethylation is required for homologous recombination repair and genome stability. *Cell Rep.*, **7**, 2006–2018.

19. Pai,C.C., Deegan,R.S., Subramanian,L., Gal,C., Sarkar,S., Blaikley,E.J., Walker,C., Hulme,L., Bernhard,E., Codlin,S. *et al.* (2014) A histone H3K36 chromatin switch coordinates DNA double-strand break repair pathway choice. *Nat. Commun.*, **5**, 4091.

20. Jha,D.K. and Strahl,B.D. (2014) An RNA polymerase II-coupled function for histone H3K36 methylation in checkpoint activation and DSB repair. *Nat. Commun.*, **5**, 3965.

21. Carvalho,S., Vitor,A.C., Sridhara,S.C., Martins,F.B., Raposo,A.C., Desterro,J.M., Ferreira,J. and de Almeida,S.F. (2014) SETD2 is required for DNA double-strand break repair and activation of the p53-mediated checkpoint. *eLife*, **3**, e02482.

22. Aymard,F., Bugler,B., Schmidt,C.K., Guillou,E., Caron,P., Briois,S., Iacovoni,J.S., Daburon,V., Miller,K.M., Jackson,S.P. *et al.* (2014) Transcriptionally active chromatin recruits homologous recombination at DNA double-strand breaks. *Nat. Struct. Mol. Biol.*, **21**, 366–374.

23. Fuchs,S.M., Kizer,K.O., Braberg,H., Krogan,N.J. and Strahl,B.D. (2012) RNA polymerase II carboxyl-terminal domain phosphorylation regulates protein stability of the Set2 methyltransferase and histone H3 di- and trimethylation at lysine 36. *J. Biol. Chem.*, **287**, 3249–3256.

24. McDaniel,S.L., Hepperla,A.J., Huang,J., Dronamraju,R., Adams,A.T., Kulkarni,V.G., Davis,I.J. and Strahl,B.D. (2017) H3K36 methylation regulates nutrient stress response in Saccharomyces cerevisiae by enforcing transcriptional fidelity. *Cell Rep.*, **19**, 2371–2382.

25. Janke,C., Magiera,M.M., Rathfelder,N., Taxis,C., Reber,S., Maekawa,H., Moreno-Borchart,A., Doenges,G., Schwob,E., Schiebel,E. *et al.* (2004) A versatile toolbox for PCR-based tagging of yeast genes: new fluorescent proteins, more markers and promoter substitution cassettes. *Yeast*, **21**, 947–962.

26. Holstege,F.C., Jennings,E.G., Wyrick,J.J., Lee,T.I., Hengartner,C.J., Green,M.R., Golub,T.R., Lander,E.S. and Young,R.A. (1998) Dissecting the regulatory circuitry of a eukaryotic genome. *Cell*, **95**, 717–728.

27. Bindea,G., Mlecnik,B., Hackl,H., Charoentong,P., Tosolini,M., Kirilovsky,A., Fridman,W.H., Pages,F., Trajanoski,Z. and Galon,J. (2009) ClueGO: a Cytoscape plug-in to decipher functionally grouped gene ontology and pathway annotation networks. *Bioinformatics*, **25**, 1091–1093.

28. Huang da,W., Sherman,B.T. and Lempicki,R.A. (2009) Bioinformatics enrichment tools: paths toward the comprehensive functional analysis of large gene lists. *Nucleic Acids Res.*, **37**, 1–13.

29. Chabbert,C.D., Adjalley,S.H., Klaus,B., Fritsch,E.S., Gupta,I., Pelechano,V. and Steinmetz,L.M. (2015) A high-throughput ChIP-Seq for large-scale chromatin studies. *Mol. Syst. Biol.*, **11**, 777.

30. Churchman,L.S. and Weissman,J.S. (2011) Nascent transcript sequencing visualizes transcription at nucleotide resolution. *Nature*, **469**, 368–373.

31. Hoffman,M.M., Buske,O.J. and Noble,W.S. (2010) The Genomedata format for storing large-scale functional genomics data. *Bioinformatics*, **26**, 1458–1459.

32. Lickwar,C.R., Rao,B., Shabalin,A.A., Nobel,A.B., Strahl,B.D. and Lieb,J.D. (2009) The Set2/Rpd3S pathway suppresses cryptic transcription without regard to gene length or transcription frequency. *PLoS One*, **4**, e4886.

33. Santos,A., Wernersson,R. and Jensen,L.J. (2015) Cyclebase 3.0: a multi-organism database on cell-cycle regulation and phenotypes. *Nucleic Acids Res.*, **43**, D1140–D1144.

34. Li,B., Gogol,M., Carey,M., Pattenden,S.G., Seidel,C. and Workman,J.L. (2007) Infrequently transcribed long genes depend on the Set2/Rpd3S pathway for accurate transcription. *Genes Dev.*, **21**, 1422–1430.

35. Dominguez,D., Tsai,Y.H., Gomez,N., Jha,D.K., Davis,I. and Wang,Z. (2016) A high-resolution transcriptome map of cell cycle reveals novel connections between periodic genes and cancer. *Cell Res.*, **26**, 946–962.

36. Hongay,C.F., Grisafi,P.L., Galitski,T. and Fink,G.R. (2006) Antisense transcription controls cell fate in Saccharomyces cerevisiae. *Cell*, **127**, 735–745.

37. Nadal-Ribelles,M., Sole,C., Xu,Z., Steinmetz,L.M., de Nadal,E. and Posas,F. (2014) Control of Cdc28 CDK1 by a stress-induced lncRNA. *Mol. Cell*, **53**, 549–561.

38. Gelfand,B., Mead,J., Bruning,A., Apostolopoulos,N., Tadigotla,V., Nagaraj,V., Sengupta,A.M. and Vershon,A.K. (2011) Regulated antisense transcription controls expression of cell-type-specific genes in yeast. *Mol. Cell. Biol.*, **31**, 1701–1709.

39. McKinney,J.D., Chang,F., Heintz,N. and Cross,F.R. (1993) Negative regulation of FAR1 at the Start of the yeast cell cycle. *Genes Dev.*, **7**, 833–843.

40. Spellman,P.T., Sherlock,G., Zhang,M.Q., Iyer,V.R., Anders,K., Eisen,M.B., Brown,P.O., Botstein,D. and Futcher,B. (1998) Comprehensive identification of cell cycle-regulated genes of the yeast Saccharomyces cerevisiae by microarray hybridization. *Mol. Biol. Cell*, **9**, 3273–3297.

41. Granovskaia,M.V., Jensen,L.J., Ritchie,M.E., Toedling,J., Ning,Y., Bork,P., Huber,W. and Steinmetz,L.M. (2010) High-resolution transcription atlas of the mitotic cell cycle in budding yeast. *Genome Biol.*, **11**, R24.

42. Castelnuovo,M., Zaugg,J.B., Guffanti,E., Maffioletti,A., Camblong,J., Xu,Z., Clauder-Munster,S., Steinmetz,L.M., Luscombe,N.M. and Stutz,F. (2014) Role of histone modifications and early termination in pervasive transcription and antisense-mediated gene silencing in yeast. *Nucleic Acids Res.*, **42**, 4348–4362.

43. Biswas,D., Takahata,S., Xin,H., Dutta-Biswas,R., Yu,Y., Formosa,T. and Stillman,D.J. (2008) A role for Chd1 and Set2 in negatively regulating DNA replication in Saccharomyces cerevisiae. *Genetics*, **178**, 649–659.

44. Pai,C.C., Kishkevich,A., Deegan,R.S., Keszthelyi,A., Folkes,L., Kearsey,S.E., De Leon,N., Soriano,I., de Bruin,R.A.M., Carr,A.M. *et al.* (2017) Set2 methyltransferase facilitates DNA replication and promotes genotoxic stress responses through MBF-dependent transcription. *Cell Rep.*, **20**, 2693–2705.

45. Dimitrova,E., Turberfield,A.H. and Klose,R.J. (2015) Histone demethylases in chromatin biology and beyond. *EMBO Rep.*, **16**, 1620–1639.

46. Pesin,J.A. and Orr-Weaver,T.L. (2008) Regulation of APC/C activators in mitosis and meiosis. *Annu. Rev. Cell Dev. Biol.*, **24**, 475–499.

47. Primorac,I. and Musacchio,A. (2013) Panta rhei: the APC/C at steady state. *J. Cell Biol.*, **201**, 177–189.

48. Hacker,K.E., Fahey,C.C., Shinsky,S.A., Chiang,Y.J., DiFiore,J.V., Jha,D.K., Vo,A.H., Shavit,J.A., Davis,I.J., Strahl,B.D. *et al.* (2016) Structure/Function analysis of recurrent mutations in SETD2 protein reveals a critical and conserved role for a SET domain residue in maintaining protein stability and histone H3 Lys-36 trimethylation. *J. Biol. Chem.*, **291**, 21283–21295.

49. Huber,F., Bunina,D., Gupta,I., Khmelinskii,A., Meurer,M., Theer,P., Steinmetz,L.M. and Knop,M. (2016) Protein abundance control by non-coding antisense transcription. *Cell Rep.*, **15**, 2625–2636.

50. Kim,J.H., Lee,B.B., Oh,Y.M., Zhu,C., Steinmetz,L.M., Lee,Y., Kim,W.K., Lee,S.B., Buratowski,S. and Kim,T. (2016) Modulation of mRNA and lncRNA expression dynamics by the Set2-Rpd3S pathway. *Nat. Commun.*, **7**, 13534.

51. Grosso,A.R., Leite,A.P., Carvalho,S., Matos,M.R., Martins,F.B., Vitor,A.C., Desterro,J.M., Carmo-Fonseca,M. and de Almeida,S.F. (2015) Pervasive transcription read-through promotes aberrant expression of oncogenes and RNA chimeras in renal carcinoma. *eLife*, **4**, e09214.

52. Park,I.Y., Powell,R.T., Tripathi,D.N., Dere,R., Ho,T.H., Blasius,T.L., Chiang,Y.C., Davis,I.J., Fahey,C.C., Hacker,K.E. *et al.* (2016) Dual chromatin and cytoskeletal remodeling by SETD2. *Cell*, **166**, 950–962.

53. Ard,R. and Allshire,R.C. (2016) Transcription-coupled changes to chromatin underpin gene silencing by transcriptional interference. *Nucleic Acids Res.*, **44**, 10619–10630.